ChemComm

N-Oxides Amplify Catalyst Reactivity and Isoselectivity in the Ring-Opening Polymerization of *rac*-β-Butyrolactone

Journal:	*ChemComm*
Manuscript ID	CC-COM-09-2021-005127.R2
Article Type:	Communication

COMMUNICATION

N-Oxides Amplify Catalyst Reactivity and Isoselectivity in the Ring-Opening Polymerization of *rac*-β-Butyrolactone

Received 00th January 20xx,
Accepted 00th January 20xx

DOI: 10.1039/x0xx00000x

Xiang Dong, Alexander M. Brown, Audra J. Woodside, Jerome R. Robinson*

_N_-oxides can amplify the performance of a lanthanum aminobisphenolate catalyst in the ring-opening polymerization (ROP) of *rac*-β-butyrolactone (*rac*-BBL) to unprecedented levels (TOF / P_m; At RT: 1,900 h^{-1} / 0.73, At –30 °C: 200 h^{-1} / 0.82). Experiments and computations establish donor electronics control catalyst activity, while donor sterics control catalyst deactivation.

Our global production, consumption, and disposal of enormous volumes of environmentally-persistent polymers is contributing to one of the greatest environmental concerns of our generation.[1] Poly-3-hydroxybutyrate (P3HB), the most common polyhydroxyalkanoate (PHA), is a naturally occurring polymer capable of degrading under ambient conditions in the environment.[3] Furthermore, P3HB can display comparable mechanical and thermal properties to that of traditional polyolefins (e.g. isotactic polypropylene), depending on composition and microstructure (e.g. tacticity).[4] Although microbial fermentation can provide access to P3HB, production costs remain high and only perfectly isotactic P3HB (percentage meso diads, P_m = 0.99) can be generated.[5]

The stereospecific ring-opening polymerization (ROP) of easily-sourced, inexpensive, racemic cyclic esters is an attractive method to access PHAs with defined microstructure.[6] High-activity catalysts capable of accessing syndioenriched P3HB have been reported,[7] yet access to isoenriched P3HB remains limited. Chen and coworkers developed an elegant strategy using 8-membered cyclic diolides to access near perfectly isotactic P3HB and stereoblock PHA copolymers;[8] however, a multi-step synthesis is required to access these monomers. Racemic β-lactones such as *rac*-β-butyrolactone (*rac*-BBL) can be derived from abundant feedstocks via epoxide carbonylation,[9] but isoselective catalysts remain rare and generally suffer from low activity under ambient conditions (turnover frequency, TOF ~4 – 25 h^{-1}).[10]

Department of Chemistry, Brown University, Providence, RI 02912, USA
Email: jerome_robinson@brown.edu
† Electronic Supplementary Information (ESI) available: DOI: 10.1039/x0xx00000x

Recently, our group discovered that incorporating increased coordinative unsaturation and ligand flexibility into rare-earth complexes can generate catalysts whose performance in the stereospecific ROP of *rac*-BBL can be amplified by addition of simple and inexpensive monodentate neutral donor ligands.[11] In the case of a lanthanum *N*-benzyl aminobisphenolate catalyst, [La(^{Bn}L)(N(SiHMe$_2$)$_2$)(THF)$_2$] (^{Bn}L: BnN(CH$_2$-2,6-t^{Bu}ArO)$_2$), **1-La**, addition of hard phosphine oxide donors (OPR$_3$; R = ^{n}C$_8$H$_{17}$, Ph, NMe$_2$) generated the most isoselective and reactive homogeneous catalysts for the ROP of *rac*-BBL reported to date (e.g. OP(^{n}C$_8$H$_{17}$)$_3$, 0 °C: TOF = ~200 h^{-1}, P_m = 0.80).[11a] Our initial mechanistic studies with OPPh$_3$ revealed that these dynamic, strong neutral donors influenced several key catalyst equilibria associated with propagation, stereocontrol, and catalyst deactivation. We posited that each of these equilibria, and therefore catalyst performance, might be uniquely attenuated by donor structure and strength. Herein, we report that another class of neutral donor ligands, *N*-oxides, can promote unprecedented amplification of catalyst activity and isoselectivity in the ROP of *rac*-BBL.

Heteroaromatic *N*-oxides are a versatile class of neutral donor ligands with exceptional structural and electronic diversity[12]. Although alkyl and heteroaromatic *N*-oxides have been employed with great success as additives and ligands in asymmetric catalysis,[14] this marks their first use in ROP. **1-La** was evaluated as a catalyst for the ROP of *rac*-BBL in the presence of diphenylmethanol (HOCHPh$_2$) and pyridine *N*-oxide derivatives (Table 1). In the absence of a strong neutral donor ligand, the La alkoxide formed *in situ* from 0.5 mol% **1-La** and HOCHPh$_2$ was modestly active with a slight preference towards formation of isoenriched P3HB (Entry 1, P_m = 0.57). Addition of pyridine *N*-oxide (PyO, 1 mol%), increased rates and isoselectivity (entry 3, P_m = 0.68), albeit less than a monodentate phosphine-oxide such as OPPh$_3$ (entry 2). Our prior studies of **1-La** supported increased catalyst performance with stronger neutral donor ligands,[11a] while increased steric congestion has played a key role in increased levels of stereocontrol in stereospecific ROP.[6b,7d] We hypothesized the

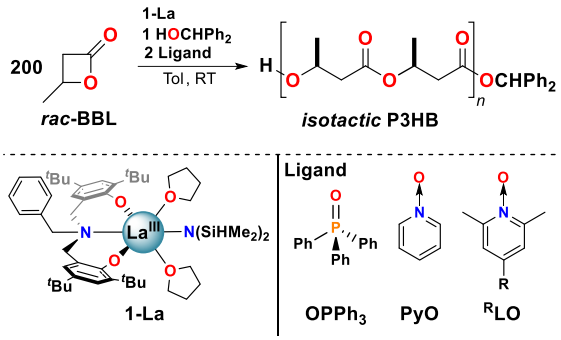

Scheme 1. Catalyst and ligands used in this study.

Table 1. ROP of *rac*-BBL (2.4 M) catalyzed by **1-La** (0.5 mol%) in the presence of $HOCHPh_2$ (0.5 mol%) and neutral donor ligands (1 mol%).

Entry	Ligand	Time (h)[a]	Conv. (%)[b]	$M_{n,calc}$[c] (kg/mol)	$M_{n,exp}$[d] (kg/mol)	$Đ$[e] (M_w/M_n)	P_m[f]
1	-	1	20	3.6	2.8	1.05	0.57
2	$OPPh_3$	1	95	16.5	9.4	1.19	0.71
3	PyO	3	55	9.7	7.1	1.14	0.68
4	^{NMe2}LO	10	22	4.0	2.2	1.23	0.72
5	^{OMe}LO	0.1	95	16.5	12.5	1.16	0.73
6	LO	0.3	92	16.0	11.4	1.18	0.73
7	^{Cl}LO	0.5	93	16.2	11.7	1.16	0.73
8	^{NO2}LO	5	31	5.5	2.2	1.28	0.69
9	^{OMe}LO[g]	1	99	17.2	15.1	1.08	0.82

a – Reaction times not optimized. *b* – Determined by ^{1}H NMR integration of BBL and P3HB methine resonances in the crude reaction mixture. *c* – $n \times 0.08609 + 0.18424$ kg/mol. *d* – Determined by gel permeation chromatography (GPC) at 30 °C in THF using polystyrene standards and corrected by a Mark-Houwink factor of 0.54.[15] *e* – M_w/M_n. *f* – Probability of *meso* linkages between repeat units. Determined by integration of P3HB *C*=O resonances using inverse gated (IG) $^{13}C\{^1H\}$ NMR. *g* – At –30 °C.

lower performance of PyO compared to $OPPh_3$ was due to differences in their stereoelectronic properties. Electronically, PyO is a weaker donor than $OPPh_3$ by the 4-fluorophenol hydrogen-bond basicity scale,[16] while buried volume calculations (%V_{bur}) support a significantly reduced steric profile for PyO relative to $OPPh_3$ (%V_{bur}(PyO): 12.4%, %V_{bur}($OPPh_3$): 16.3%; Table S30 and S31). Alternatively, 4-substituted 2,6-dimethylpyridine (lutidine) *N*-oxide derivatives, ^{R}LO (R = NO_2, Cl, H, OMe, NMe_2), display steric profiles comparable to $OPPh_3$ (Table S32; %V_{bur}: 15.9%), while experimental aqueous pK_a values (pK_a^W(^{NO2}LO): 1.01, pK_a^W(^{NMe2}LO): 4.75)[17] and calculated natural charges of the *N*-oxide oxygen (q_O(^{NO2}LO): –0.541, q_O(^{NMe2}LO): –0.658; Figure S15 & Table S6) support electronically tunable donor profiles.

Consistent with this hypothesis, ^{R}LO had a significant impact on catalyst activity and selectivity. Catalyst isoselectivity generally increased for ^{R}LO relative to PyO, and was nearly invariant with respect to donor strength (Table 1, entries 4–8; P_m = 0.69–0.73). In contrast, catalyst TOF varied ~430-fold, where peak values occurred with an *N*-oxide of *intermediate* donor strength, ^{OMe}LO (Figure S9). The overall trend in activity was reminiscent of volcano plots[18] following Sabatier's principle.[19] Such effects are frequently encountered in heterogeneous systems, but only recently observed in homogeneous catalysis.[20] At RT, ^{OMe}LO promoted a 10-fold increase in activity compared to the previous champion system (**1-La** / L; TOF(^{OMe}LO) ~1,900 h^{-1} *vs* TOF($OPPh_3$) ~200 h^{-1}). Similar to $OPPh_3$, improvements in catalyst activity and selectivity saturate at two equiv of ^{OMe}LO (Table S2; 0 – 3 equiv ^{OMe}LO). Lowering the reaction temperature to –30 °C led to improved isoselectivity while maintaining high catalyst activity (entry 9: P_m = 0.82, TOF ~200 h^{-1}).

Insight into the mechanism of catalyst initiation and propagation was obtained from binding studies of **1-La** in the presence of $HOCHPh_2$ (one equiv), ^{OMe}LO (one or two equiv), and γ-butyrolactone (GBL; 0 – 100 equiv), as well a end-group analysis of P3HB produced from **1-La**:$HOCHPh_2$:^{OMe}LO:*rac*-BBL (1:1:2:200). GBL was used in ^{1}H NMR binding studies as it is stereoelectronically similar to *rac*-BBL, yet unpolymerizable at RT. ^{1}H NMR revealed formation of effectively identical La species with ≥ 10 equiv GBL and one or two equiv ^{OMe}LO (Figure S13 and S14). This was consistent with the major La species as mono-^{OMe}LO bound and analogous to mono-$OPPh_3$ species observed with **1-La**.[11a] Alternatively, direct association of *rac*-BBL to form a seven-coordinate La species was predicted to be favorable based on DFT calculations at the rM06-L level of theory (Figure S20). Taken together, these studies support ligand exchange during initiation is not rate-determining, and that both six- and seven-coordinate species should be considered as plausible initiating species. End-group analysis of P3HB using ^{1}H NMR spectroscopy revealed the presence of ester and alcohol end-groups in a ~1:1 ratio (Figure S5), and unambiguously established a coordination-insertion mechanism (i.e. acyl cleavage).[21] Notably, crotyl end-groups were nearly undetectable (< ~0.02 equiv / -$OCHPh_2$), indicative that *N*-oxide binding suppressed base-promoted elimination to a much greater extent than *P*-oxide donors (e.g. $OPPh_3$: 1 equiv / **1-La**).[11a] This was further corroborated by the excellent agreement between experimental and calculated M_n and narrow $Đ$ maintained throughout the reaction (Figure S8).

Previously, we discovered that strong neutral donor ligands could amplify catalyst performance in the ROP of *rac*-BBL by (i) suppressing catalyst deactivation and (ii) increasing propagation rates.[11a,b] However, it was not possible to fully decouple the influence of donors on each of these steps. Propagation rates (k_p) devoid of contributions from catalyst deactivation and uncontrolled reaction exotherms were obtained from kinetic studies performed with **1-La** (1 mol%) and

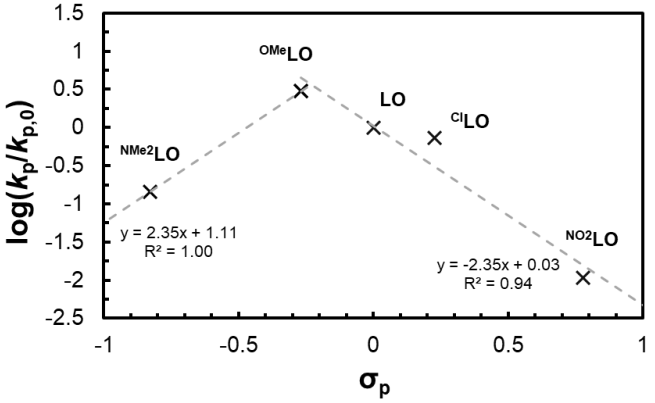

Figure 2. Hammett plot of log($k_p/k_{p,0}$) *vs* σ_p for the ROP of *rac*-BBL (0.3 M) catalyzed by **1-La**:$HOCHPh_2$:^{R}LO (1:1:2 mol%) in toluene at RT. k_p: propagation rate of ^{R}LO. $k_{p,0}$: k_p of LO. σ_p: Hammett para-substituent constant.

^{R}LO or $OPPh_3$ (2 mol%) at RT under more dilute conditions (0.3 M *vs* 2.4 M; see Supporting Information). A Hammett plot of k_p for ^{R}LO normalized to the parent LO ($\log(k_p/k_{p,0})$) revealed a strong rate dependence on donor electronics with a 290-fold change in k_p moving from ^{NO2}LO to ^{OMe}LO (Figure 2). A ρ value of ~–2.4 was obtained from the slope of $\log(k_p)$ values containing ^{NO2}LO to ^{OMe}LO, and indicated a significant build-up of positive charge in the transition-state of the turnover limiting step. Furthermore k_p dropped dramatically with the most electron-rich ^{R}LO, ^{NMe2}LO, indicative of a mechanism changeover. Although further work is needed, these studies reveal that donor association is rate-limiting for weak and intermediate donors, ^{NO2}LO–^{OMe}LO, while donor dissociation becomes rate-limiting for the strongest donor, ^{NMe2}LO, during propagation.

Given the unprecedented reactivity of **1-La** in the presence of $HOCHPh_2$ and ^{R}LO, we set out to characterize the metal-ligand adducts to better understand catalyst performance. A 1:2 binding stoichiometry between [**La**]:[^{OMe}**LO**] was determined following the titration of **1-La** with varying equivalents of ^{OMe}LO (0 – 3 equiv) using ^{1}H NMR spectroscopy (Figure S11). Isolation of the 1:2 adducts, [La(^{Bn}L)($OCHPh_2$)(^{OMe}LO)$_2$] (**2-La(^{OMe}LO)$_2$**) and [La(^{Bn}L)($OCHPh_2$)($OPPh_3$)$_2$] (**2-La($OPPh_3$)$_2$**), were achieved in 88% and 91% yield, respectively, from the protonolysis of H^{Bn}L by La[N(SiHMe$_2$)$_2$]$_3$(THF)$_2$ followed by two equivalents ^{OMe}LO or $OPPh_3$. Similar to **1-La($OPPh_3$)**, ^{1}H Diffusion-ordered NMR spectroscopy (DOSY)[23] supported monomeric formulations of **2-La(^{OMe}LO)$_2$** and **2-La($OPPh_3$)$_2$** in C_6D_6 (Figure S3 and S4). The number and integration of ^{1}H NMR resonances corresponding to ^{Bn}L, $OCHPh_2$, and ^{OMe}LO or $OPPh_3$ supported effective C_s symmetry in solution, and was indicative of free rotation about the La–O_{CHPh2} bond and rapid exchange of the axial neutral donor-ligands on the NMR timescale. Quantification of free- and bound-$OPPh_3$ using inverse-gated ^{31}P NMR generated the following series: ^{NMe2}LO > ^{OMe}LO > $OPPh_3$ ~ LO > ^{Cl}LO >> ^{NO2}LO (Figure S12, Table S5), where donor order followed expectations based on pK_a, σ_p, and natural charge of free ^{R}LO (*vide supra*). Furthermore, $OPPh_3$ and LO displayed comparable binding affinities, which made these ideal pairs to delineate the effects of donor sterics on catalyst performance.

Further insight was provided by DFT modelling studies of the $OPPh_3$ and LO adducts of amide and alkoxide precatalysts (**1-La(L)$_2$** and **2-La(L)$_2$**; L = $OPPh_3$ and LO). For brevity, the discussion will focus on **1-La(L)$_2$**, as similar trends were observed for **1-La(L)$_2$** and **2-La(L)$_2$** (see Supporting Information). The optimized structure of **1-La($OPPh_3$)$_2$** obtained at the rM06-L[24] level of theory with Grimme's D3 dispersion correction[25] using Stuttgart-Dresden effective core-potentials on La[26] and 6-31G*[27] as a basis set for all other atoms was in good agreement with the previously reported X-ray structure (mean unsigned error, MUE: 0.0465, Table S20). Partial space-filling models of **1-La(L)$_2$** revealed that LO and $OPPh_3$ exert significant axial steric pressure at the catalyst reaction site(Figure 3), and the planar LO donor can adopt a similar conformation to the $OPPh_3$ phenyl rings positioned closest to the reaction site. Natural population analysis performed with NBO 3.1[28] revealed negligible differences in the natural charge of the amido nitrogen

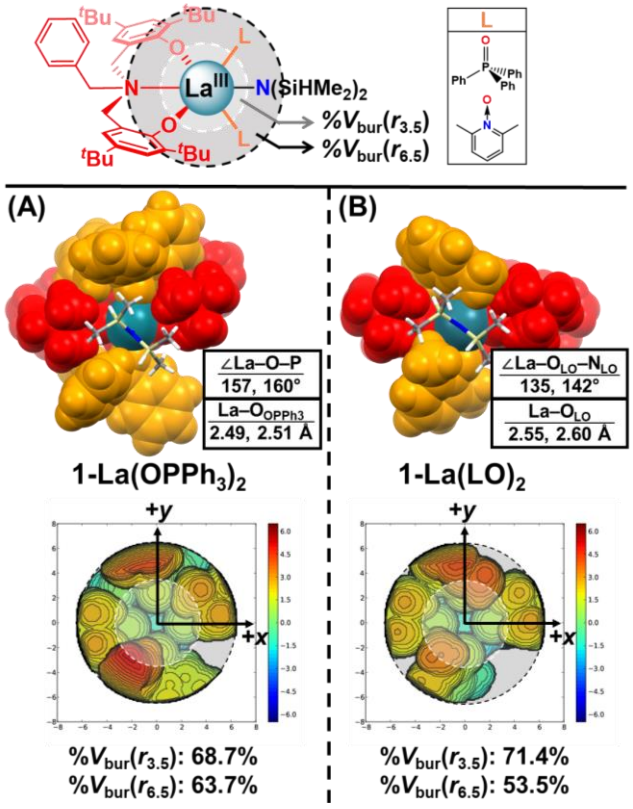

Figure 3. Comparison of DFT-optimized structures of (A) **1-La($OPPh_3$)$_2$** and (B) **1-La(LO)$_2$**. Space-filling diagram: Neutral donors ($OPPh_3$, LO; orange), ^{Bn}L (red), La^{III} (teal). Capped sticks: N(SiHMe$_2$)$_2$. Buried volume (%V_{bur}) calculated at a radius (r) of 3.5 (white) and 6.5 Å (gray). La and N(SiHMe$_2$)$_2$ were excluded from the %V_{bur} calculations.

($q_{\underline{N}(SiHMe2)2}$: **1-La($OPPh_3$)$_2$** = –1.84, **1-La(LO)$_2$** = –1.85), and implied steric origins for their differing performance.

Buried volumes calculated using Samb*V*ca 2.1[29] revealed distinct and opposite crowding effects for LO and $OPPh_3$ in the primary and secondary coordination spheres. (Figure 3 and Table S39–S42). For LO, the ortho methyl groups and shallow La–O_{LO}–N_{LO} bond-angles increased steric pressure within the primary coordination sphere (%V_{bur}($r_{3.5}$): **1-La($OPPh_3$)$_2$** = 63.7%, **1-La(LO)$_2$** = 68.7%), which may disfavour coordination of P3HB ester linkages and limit/suppress base-promoted elimination. Alternatively, the aryl groups of $OPPh_3$ increased steric crowding in the secondary coordination sphere (%V_{bur}($r_{6.5}$): **1-La($OPPh_3$)$_2$** = 71.4%, **1-La(LO)$_2$** = 53.5%), yet minimally impacted selectivity and rates.

In closing, *N*-oxides can amplify catalyst performance in stereospecific ROP to unprecedented levels, where addition of ^{OMe}LO to **1-La** generates the most active isoselective catalyst for the ROP of *rac*-BBL reported to date. Our studies begin to establish clear connections between donor structure and strength on catalyst performance. The turnover limiting step is sensitive to ligand binding equilibria, where donor strength gates catalyst activity. Alternatively, donor steric profile in the primary coordination sphere plays a role in suppressing catalyst deactivation. While the presence of a donor is crucial to the observed stereoselectivity, P_m were found to be nearly independent of donor strength and steric profile. These results suggest that further improvements in catalyst performance

might be realized by varying donor steric profile in the primary coordination sphere while optimizing binding affinity.

This research was supported by Brown University and AJW was supported by the National Science Foundation Graduate Research Fellowship (Grant No. 2040433). We thank Mehmed Z. Ertem, Jonathan E. Chellali, and Kerry C. Casey for helpful discussions. Combustion analysis was obtained from the CENTC Elemental Analysis Facility at the University of Rochester, funded by NSF CHE-0650456. There are no conflicts to declare.

Notes and references

1. R. Geyer; J. R. Jambeck; K. L. Law, *Sci. Adv.* **2017,** *3*, e1700782.
2. (a) X. Zhang; M. Fevre; G. O. Jones; R. M. Waymouth, *Chem. Rev.* **2018,** *118*, 839-885; (b) G. W. Coates; Y. D. Y. L. Getzler, *Nat. Rev. Mat.* **2020,** *5*, 501-516; (c) D. E. Fagnani; J. L. Tami; G. Copley; M. N. Clemons; Y. D. Y. L. Getzler; A. J. McNeil, *ACS Macro Lett.* **2021,** *10*, 41-53.
3. R. W. Lenz; R. H. Marchessault, *Biomacromolecules* **2005,** *6*, 1-8.
4. M. Haslböck; M. Klotz; J. Sperl; V. Sieber; C. Zollfrank; D. Van Opdenbosch, *Macromolecules* **2019,** *52*, 5407-5418.
5. B. Rieger; A. Künkel; G. W. Coates; R. Reichardt; E. Dinjus; T. A. Zevaco, Synthetic Biodegradable Polymers. Springer Berlin: Berlin, 2014; pp 49-90.
6. (a) J.-F. Carpentier, *Macromol. Rapid Commun.* **2010,** *31*, 1696-1705; (b) C. M. Thomas, *Chem. Soc. Rev.* **2010,** *39*, 165-173.
7. (a) A. Amgoune; C. M. Thomas; S. Ilinca; T. Roisnel; J.-F. Carpentier, *Angew. Chem. Int. Ed.* **2006,** *45*, 2782-2784; (b) J. Fang; M. J. L. Tschan; T. Roisnel; X. Trivelli; R. M. Gauvin; C. M. Thomas; L. Maron, *Polym. Chem.* **2012,** *4*, 360-367; (c) J. S. Klitzke; T. Roisnel; E. Kirillov; O. d. L. Casagrande; J.-F. Carpentier, *Organometallics* **2014,** *33*, 309-321; (d) J.-F. Carpentier, *Organometallics* **2015,** *34*, 4175-4189.
8. (a) X. Tang; E. Y. X. Chen, *Nat. Commun.* **2018,** *9*, 1-11; (b) X. Tang; A. H. Westlie; E. M. Watson; E. Y. X. Chen, *Science* **2019,** *366*, 754; (c) X. Tang; A. H. Westlie; L. Caporaso; L. Cavallo; L. Falivene; E. Y.-X. Chen, *Angew. Chem. Int. Ed.* **2020,** *59*, 7881-7890.
9. Y. D. Y. L. Getzler; V. Mahadevan; E. B. Lobkovsky; G. W. Coates, *J. Am. Chem. Soc.* **2002,** *124*, 1174-1175.
10. (a) D. E. Agostini; J. B. Lando; J. R. Shelton, *J. Polym. Sci. A Polym. Chem.* **1971,** *9*, 2775-2787; (b) S. Bloembergen; D. A. Holden; T. L. Bluhm; G. K. Hamer; R. H. Marchessault, *Macromolecules* **1989,** *22*, 1656-1663; (c) M. Zintl; F. Molnar; T. Urban; V. Bernhart; P. Preishuber-Pflügl; B. Rieger, *Angew. Chem. Int. Ed.* **2008,** *47*, 3458-3460; (d) N. Ajellal; G. Durieux; L. Delevoye; G. Tricot; C. Dujardin; C. M. Thomas; R. M. Gauvin, *Chem. Commun.* **2010,** *46*, 1032-1034; (e) Z. Zhuo; C. Zhang; Y. Luo; Y. Wang; Y. Yao; D. Yuan; D. Cui, *Chem. Commun.* **2018,** *54*, 11998-12001.
11. (a) X. Dong; J. R. Robinson, *Chem. Sci.* **2020,** *11*, 8184-8195; (b) K. C. Casey; J. K. Appiah; J. R. Robinson, *Inorg. Chem.* **2020,** *59*, 14827-14837; (c) X. Dong; J. R. Robinson, *New Journal of Chemistry* **2022,** *46*, 444-453.
12. (a) N. M. Karayannis; L. L. Pytlewski; C. M. Mikulski, *Coord. Chem. Rev.* **1973,** *11*, 93-159; (b) N. M. Karayannis; A. N. Speca; D. E. Chasan; L. L. Pytlewski, *Coord. Chem. Rev.* **1976,** *20*, 37-80; (c) Y. Wang; L. Zhang, *Synthesis* **2015,** *47*, 289-305.
13. (a) E. P. Buchikhin; A. M. Chekmarev; Y. A. Agafonov; A. V. Ulanov; A. Y. Kuznetsov, *Russ. J. Gen. Chem.* **2002,** *72*, 1049-1052; (b) C. Laurence; J.-F. Gal, The Donor Number or SbCl5 Affinity Scale. In *Lewis Basicity and Affinity Scales*, 2009; pp 71-83.
14. (a) R. Irie; Y. Ito; T. Katsuki, *Synlett* **1991,** *1991*, 265-266; (b) E. N. Jacobsen; W. Zhang; A. R. Muci; J. R. Ecker; L. Deng, *J. Am. Chem. Soc.* **1991,** *113*, 7063-7064; (c) R. I. Kureshy; N. H. Khan; S. H. R. Abdi; A. K. Bhatt; P. Iyer, *J. Mol. Catal.* **1997,** *121*, 25-31; (d) W. Adam; C. Mock-Knoblauch; C. R. Saha-Möller; M. Herderich, *J. Am. Chem. Soc.* **2000,** *122*, 9685-9691; (e) F.-X. Chen; H. Zhou; X. Liu; B. Qin; X. Feng; G. Zhang; Y. Jiang, *Chem. Eur. J.* **2004,** *10*, 4790-4797; (f) X. Liu; L. Lin; X. Feng, *Acc. Chem. Res.* **2011,** *44*, 574-587; (g) X. Liu; H. Zheng; Y. Xia; L. Lin; X. Feng, *Acc. Chem. Res.* **2017,** *50*, 2621-2631.
15. M. Save; M. Schappacher; A. Soum, *Macromol. Chem. Phys.* **2002,** *203*, 889-899.
16. C. Laurence; J.-F. Gal, Thermodynamic and Spectroscopic Scales of Hydrogen-Bond Basicity and Affinity. In *Lewis Basicity and Affinity Scales*, 2009; pp 111-227.
17. (a) Z. Dega-Szafran; M. Grundwald-Wyspiańska; A. Kania; Z. Kosturkiewicz; E. Tykarska; M. Szafran, *J. Mol. Struct.* **1995,** *356*, 169-182; (b) Ł. Gurzyński; A. Puszko; M. Makowski; L. Chmurzyński, *J. Chem. Thermodyn.* **2007,** *39*, 309-315.
18. (a) R. Parsons, *J. Chem. Soc. Faraday Trans.* **1958,** *54*, 1053-1063; (b) H. Gerischer, *Bull. Soc. Chim. Belg.* **1958,** *67*, 506-527.
19. P. Sabatier, *Chem. Ber.* **1911,** *44*, 1984-2001.
20. (a) G. F. Swiegers, *Mechanical Catalysis: Methods of Enzymatic, Homogeneous, and Heterogeneous Catalysis*. John Wiley & Sons: Hoboken, NJ, 2008; (b) M. Busch; M. D. Wodrich; C. Corminboeuf, *Chemical Science* **2015,** *6*, 6754-6761; (c) M. D. Wodrich; B. Sawatlon; M. Busch; C. Corminboeuf, *Accounts of Chemical Research* **2021,** *54*, 1107-1117.
21. (a) C. Lavallee; D. Grenier; R. E. Prud'homme; A. Leborgne; N. Spassky, Synthesis and Properties of Racemic and Optically Active Substituted Poly(β-Propiolactones). In *Advances in Polymer Synthesis*, B. M. Culbertson; J. E. McGrath, Eds. Springer US: Boston, MA, 1985; pp 441-460; (b) Y. Zhang; R. A. Gross; R. W. Lenz, *Macromolecules* **1990,** *23*, 3206-3212.
22. (a) H. R. Kricheldorf; N. Scharnagl; Z. Jedlinski, *Polymer* **1996,** *37*, 1405-1411; (b) L. R. Rieth; D. R. Moore; E. B. Lobkovsky; G. W. Coates, *J. Am. Chem. Soc.* **2002,** *124*, 15239-15248.
23. (a) K. F. Morris; C. S. Johnson, *J. Am. Chem. Soc.* **1992,** *114*, 3139-3141; (b) I. Keresztes; P. G. Williard, *J. Am. Chem. Soc.* **2000,** *122*, 10228-10229; (c) P. S. Pregosin, NMR diffusion methods in inorganic and organometallic chemistry. In *Spectroscopic Properties of Inorganic and Organometallic Compounds: Techniques, Materials and Applications, Volume 42*, The Royal Society of Chemistry: 2012; Vol. 42, pp 248-268.
24. Y. Zhao; D. G. Truhlar, *J. Chem. Phys.* **2006,** *125*, 194101.
25. S. Grimme; J. Antony; S. Ehrlich; H. Krieg, *J. Chem. Phys.* **2010,** *132*, 154104.
26. (a) M. Dolg; H. Stoll; A. Savin; H. Preuss, *Theoret. Chim. Acta* **1989,** *75*, 173-194; (b) M. Dolg; H. Stoll; H. Preuss, *Theoret. Chim. Acta* **1993,** *85*, 441-450.
27. (a) G. A. Petersson; A. Bennett; T. G. Tensfeldt; M. A. Al-Laham; W. A. Shirley; J. Mantzaris, *J. Chem. Phys.* **1988,** *89*, 2193-2218; (b) G. A. Petersson; M. A. Al-Laham, *J. Chem. Phys.* **1991,** *94*, 6081-6090; (c) V. A. Rassolov; J. A. Pople; M. A. Ratner; T. L. Windus, *J. Chem. Phys.* **1998,** *109*, 1223-1229.
28. A. E. R. E.D. Glendening, J.E. Carpenter, F. Weinhold, , *TCI ,University of Wisconsin, Madison,* **1998**.
29. L. Falivene; Z. Cao; A. Petta; L. Serra; A. Poater; R. Oliva; V. Scarano; L. Cavallo, *Nat. Chem.* **2019,** *11*, 872-879.

